An ice-core record of net snow accumulation and seasonal snow chemistry at Mount Waddington, southwest British Columbia, Canada

Peter D. Neff[1], Eric J. Steig[1], Douglas H. Clark[2], Joseph R. McConnell[3], Erin C. Pettit[4]

[1] Department of Earth and Space Sciences, University of Washington, Seattle, WA, USA 98195
[2] Department of Geology, Western Washington University, Bellingham, WA, USA 98225
[3] Division of Hydrologic Sciences, Desert Research Institute, Reno NV, USA 89512
[4] Department of Geology and Geophysics, University of Alaska Fairbanks, Fairbanks, AK, USA 99775

A 141m-deep ice-core was retrieved from Combatant Col (51.39° N, 125.22° W, 3000m), Mount Waddington, Coast Mountains, British Columbia, Canada. Records of black carbon, dust, lead, and water stable-isotopes show that unambiguous seasonality is preserved throughout the core, despite summer surface snowmelt and temperate ice. High accumulation rates at the site (in excess of 5 m a^{-1}) limit modification of annual stratigraphy by percolation of surface meltwater. The depth age scale for the ice-core provides sufficient constraint on the vertical strain to allow estimation of the age of the ice at bedrock. Total ice thickness at Combatant Col is ~250m; an ice-core to bedrock would likely contain ice in excess of 200 years in age. Correlation between ice flow-corrected annual snow accumulation at the site and regional precipitation using the ERA-40 and ERA-Interim global atmospheric reanalyses shows that accumulation at Combatant Col reflects regional to large-scale precipitation variability.

Introduction

Numerous ice-core records have been obtained from polar ice sheets and high-altitude tropical glaciers, and are well known for the paleoclimate information they contain (Thompson and others, 1995; Taylor and others, 1997; Fisher and others, 1998; EPICA, 2004). Ice-core records have also been obtained at mid-latitude sites, which provide information on local sources of anthropogenic and natural aerosols as well as records of regional climate that extend centuries beyond that provided by instrumental records (Schwikowski and others, 1999; Thompson, 2004; Rupper and others, 2004; Osterberg and others, 2008).

The number of mid-latitude sites suitable for ice-cores is limited, and nearly all existing records have been retrieved from just two areas: the coastal ranges of Alaska and the Yukon, and the European Alps. North American ice-core sites include Eclipse Icefield

and several sites at Mt. Logan, Yukon (Yalcin and Wake, 2001; Shiraiwa and others, 2003; Fisher and others, 2008), and Bona-Churchill Col and Mt. Wrangell, Alaska (Urmann, 2009; Yasunari and others, 2007). Ice-core sites in the European Alps include Fiescherhorn glacier (Schwikowski and others, 1999), Colle Gnifetti glacier (Thevenon and others, 2009), and Col du Dome (Vincent and others, 1997; Preunkert and others, 2000).

All of these ice-cores were obtained from cold glaciers. Sub-freezing ice temperatures are generally assumed to be essential for preservation of annual stratigraphy, and the difficulty of obtaining reliable data from temperate glacier sites is frequently noted in the literature (Naftz and others, 1996; Koerner, 1997; Schotterer and others 1997, 2004). Consequently, few ice-cores have been obtained from temperate glaciers. Even at sites where the mean annual surface temperature is well below freezing, if summer surface melting occurs, infiltration of meltwater through the snow and firn may compromise or eliminate seasonal stratigraphy. However, once snowfall is transformed through firn to solid glacial ice, little further alteration should be expected, because ice is highly impermeable (Lliboutry, 1971). This suggests that at sites where surface melting occurs, it is the degree of meltwater infiltration through the firn, rather than the temperature of the ice, that is critical to the preservation of annual stratigraphy. Ice-cores with intact annual stratigraphy may therefore be retrievable from certain temperate glaciers, provided the accumulation rate exceeds the infiltration depth. We explore this idea in the Coast Mountains of British Columbia, a region characterized by very high precipitation rates and a number of high-elevation sites with ice thicknesses greater than 200 m.

Here, we report results of an ice-core from Combatant Col (51.39° N, 125.22° W, 3000m elevation), which is a broad, nearly flat icefield in the Waddington Range, southern

Coast Mountains (Figures 1 and 2). We demonstrate that there is unambiguous seasonal stratigraphy preserved in the visual and chemical records from the ice-core, and that we can date annual-layers to a precision of ± 1 year. The resulting accumulation history is comparable to precipitation records from regional weather stations and its covariance with climate reanalysis data is consistent with understanding of large-scale controls on precipitation in this region (e.g. Overland and Hiester, 1980; Rodionov and others, 2007). We also show that, although we obtained a core through only sixty percent of the ice thickness at the site, the ice-core depth-age relationship strongly constrains the vertical strain due to ice-flow, providing sufficient information to estimate the age of the ice at bedrock. Ice within ~20 m of the bed is very likely to be in excess of 200 years in age. Because of Combatant Col's location at the southern extreme of the dipole pattern in precipitation along the coast of western North America (e.g. Bitz and Battisti, 1999), information from a deeper ice-core at this site would provide a useful complement to existing records from Alaska and the Yukon.

Ice-core collection and analysis

Ice at Combatant Col flows from a 4 km^2 plateau through two large icefalls on opposing sides, feeding ice to Tiedemann Glacier to the southeast and Scimitar Glacier to the northwest (Figure 2). A remote weather station maintained by the University of Northern British Columbia, located alongside Tiedemann Glacier 4 km southeast and 1 km below Combatant Col, indicates mean annual temperatures of -5ºC at the ice-core site (assuming a wet adiabatic lapse rate of 7 ºC km^{-1}; Peter Jackson, unpublished). Preliminary coring at the site, conducted in September 2006 to a depth of 65m, suggested annual accumulation rates of

3-5m ice-equivalent, and demonstrated preservation of seasonal cycles in soluble and insoluble chemical species throughout the firn and into the uppermost glacier ice. Radar data collected in 2007 and 2010 indicate an ice thickness of at least 230m (Figure 3).

The 141m Combatant Col ice-core was drilled in July 2010 using the Ice Drilling and Design Office (IDDO) 10-cm diameter electromechanical drill (formerly called the "PICO drill") to a depth of 55 m, and the IDDO 8-cm diameter electrothermal drill from 55 m to 141 m (Ice Drilling Design and Operations, 2011). Thermal drilling became necessary once the presence of water in the borehole prevented evacuation of drill chips in the electromechanical drill sonde. We measured the temperature of the ice with a thermal probe inserted into a small hole drilled in the side of each core retrieved within 5 minutes of retrieval; ice at the site was measured to be between -3 ºC and 0 ºC at depths below 20 m (Fig. 3c), with consistent temperatures of 0 ± 1 ºC below 40m. The region of transition from cold to temperate ice is clearly visible in the radar stratigraphy at 40 m depth, because the temperate firn is water saturated at this level (Figure 3a). The firn-ice transition at 830 g cm^{-3} occurs at ~45 m depth, based on density measured by weighing samples of each ~1 m length of core (see below). Freezing of water in the borehole below 80 m depth resulted in partial closure of the borehole over hour- to day-long periods (for example, 2 cm of refrozen ice on the borehole wall developed during a 48-hour drilling shutdown period). The addition of ethanol to the water in the borehole did not improve drilling progress, despite efforts to ensure consistent delivery of ethanol past the porous firn layers and to mix water and ethanol in the borehole thoroughly. This complication stalled drilling progress at 118 m. Efforts to continue resulted in a diversion of the borehole at ~113.5 m, as variance in drill-tower leveling made reopening and precisely following the previously-drilled borehole

impossible. The divergent borehole (~2-3° departure from initial borehole) reached a final depth of 141 m, after a second diversion at 124 m. We collected overlapping sections of ice at both borehole diversions, in order to recover accurate depth information that was lost when continuous ice-core collection was interrupted. Matching of chemical stratigraphy allowed for recovery of absolute depth correct to within a few centimeters. No further progress could be made below 141 m due to continued refreezing of water in the borehole, leaving approximately 100m of ice between the final ice-core depth and the bedrock below.

In the field, one-meter ice-core sections were cut, measured, photographed, placed in high-density polyethylene (HDPE) bags, and stored in a covered snow pit for up to four days, then taken by a ~30 minute helicopter flight to a freezer truck. At the end of the drilling season (~30 days), the ice was shipped to storage facilities at the University of Washington in Seattle. In November 2010, the core sections were shipped to the U.S. National Ice Core Laboratory in Denver, Colorado for sampling and allocation to laboratories. Core sections were cut into five parallel longitudinal samples: a center core sample (3.5cm x 3.5cm x ~1m) for chemical measurements, a side sample for water stable-isotope analysis, and several archive samples. Immediately prior to sampling, a slab of ice from the center of each core section was planed and scanned using a high-resolution digital imaging system (McGwire and others, 2008).

The ice-core was sampled continuously from the surface snow (0m) to the deepest ice (141m). We analyzed 3.5 cm x 3.5 cm x 1 m samples from the center of the core at the Desert Research Institute (DRI) using a continuous-flow analysis system (McConnell and others, 2002; McConnell and others, 2007). Ice samples are melted vertically using a sectioned heating element, isolating the innermost ice from the sample and discarding contaminated

outer surfaces. The DRI system employs two high-resolution inductively coupled plasma mass spectrometers for elemental determinations, laser-based instruments for measurements of black carbon and insoluble dust particles concentrations and size distributions, and a range of fluorimeters and spectrophotometers for chemical measurements. This instrumentation yielded <1 cm effective depth resolution measurments of continental dust indicators, sea salt, volcanism, biomass burning, and industrial pollutants in the Combatant Col core. Insoluble dust data presented here represent particle sizes of 2.4 to 4.5 nm. Results from the black carbon, lead, and dust measurements, which all exhibit clear seasonality, will be discussed in this paper. Density measurements were taken on each 3.5 cm x 3.5 cm x ~1 m core sample, by weighing and measuring dimensions; estimated uncertainty is ± 10%. A density-depth profile was estimated from these data using a third-order polynomial fit (Fig. 3b), which we use to calculate the ice-equivalent depth and thickness of annual-layers in the ice-core.

At the University of Washington stable-isotope laboratory, we cut 1416 samples at approximately 10 cm resolution for the length of the core, to be used for water stable-isotope ($\delta^{18}O$ and δD) analysis. This sampling resolution results in an average of 35 samples per year. Each sample was melted, decanted into a 20 mL HDPE bottle, and refrigerated until analysis. Measurements of $\delta^{18}O$ and δD were made simultaneously for every 10cm sample using a Picarro cavity ring-down spectrometer.

Seasonality in chemical records

Chemical records from the Combatant Col ice-core exhibit unambiguous seasonal extremes, coincident in black carbon, dust, lead, and water stable-isotopes. Peaks in all

species occur in sections of core with higher incidence of melt layers, most obviously in the snow/firn section of the core (0-40 m), but do not appear to be preferentially concentrated in individual melt layers. An example annual sequence from 17 to 21 m depth is shown in Figure 4.

Black carbon, dust and lead in the ice-core demonstrate strong seasonality (5- to 10-fold fluctuation in concentrations; Figure 4c, d, e). Black carbon concentrations range from 0 to 23.94 parts per billion (ppb) (2.4 ppb standard deviation), while minima typically range from only 0.1 ppb to 1.0 ppb (Figure 4c). Dust concentrations range from 0 to 0.68 ppb (0.03 ppb standard deviation), and show several extremely large peaks with concentrations up to 0.4 ppb, while other maxima are as low as 0.05 ppb (Figure 4d). Dust minima are less than 0.02 ppb in all cases. The record of lead from Combatant Col exhibits concentrations ranging from 0 to 2.65 ppb (0.11 ppb standard deviation). Maximum concentrations are observed in the deepest 20 m of the core (121-141 m), with peaks as high as 2 ppb and typical peak values of 0.5 ppb, compared to peak values of ≤0.4 ppb in the upper 120 m (Figure 4e). Stable-isotope concentrations ($\delta^{18}O$) vary from more negative (-22‰ to -25‰) values in the melt-free portion, to less negative (-18‰ to -14‰) in the melt-rich snow and ice (Figure 4f).

We interpret the sequence shown in Figure 4 as follows. Beginning in melt-free and impurity-poor winter snow at the base of this annual-layer, we observe gradual increases up-core (and thus through time) of all chemical species, building towards maximum concentrations and the presence of surface melt layers formed during spring and summer. Because maximum precipitation in coastal British Columbia occurs from October to March (1971-2000 climatology; Environment Canada, 2011), we interpret the deeper portion of the sequence in Figure 4 as a package of snow deposited during these winter months. The

increasingly impurity-rich upper portion of this snow sequence indicates the gradual addition of impurities to the developing snowpack, coincident with spring and summer months of warmer surface air temperatures and maximum trans-Pacific dust and pollutant fluxes from Asia (Merrill and others, 1989; Bey and others, 2001). Individual trans-Pacific transport events have been observed with diverse compositions; sometimes with components exclusively of industrial origin, though more they comprise mixes of industrial emission and mineral dust sources (Jaffe and others, 2003). Local contributions of these aerosols are likely also important, considering that Vancouver, British Columbia is only 280 km distant. Local forest fires may also contribute to the seasonal maximum in black carbon. Finally, occasional storm activity in summer deposits small amounts of snow with high impurity content and less negative $\delta^{18}O$ and δD values. The seasonality in isotopes is consistent with data compiled by Bowen (2008) from the IAEA/WMO Global Network of Isotopes in Precipitation (GNIP) stations and other sources, showing that there is strong seasonality in water isotopes along coastal British Columbia (largely due to the temperature effect).

Maximum temperatures during summer months (June-August) partially melt surface snow layers—which were deposited in winter and spring—and meltwater from these layers penetrates into the snowpack. Due to extremely high accumulation rates at Combatant Col, this meltwater penetrates only part way through an annual-layer. Thus, the seasonal cycle of water stable-isotope values and impurity concentrations is preserved. This interpretation of spring/summer stratigraphic horizon formation is the basis for our annual dating of the ice-core.

Dating

Dating of the core was performed iteratively using a multiparameter approach; adding independent data sets sequentially after counting subjectively-determined annual peaks. The visual, geochemical and isotope stratigraphy are plotted versus the final age-scale in Figure 5. Initial age-scales were developed using the records of melt layers, black carbon, and dust only. We quantitatively analyzed melt layers in the ice-core by averaging the grayscale pixel intensity of the approximate longitudinal centerline from every core section image taken during laboratory sampling. This record of pixel intensity clearly demarks transparent, bubble-free melt features as dark horizons, due to the black background and overhead lighting of the imaging system we used. Clean winter snow and firn scatters the overhead lighting and appears very bright. Visual analysis was helpful in dating the snow and firn section of the core, showing that closely spaced high-concentration excursions represent individual spring/summer aerosol deposition events. In the glacier ice below 40 m, quantitative visual analysis was not as useful because of reduced contrast between melt layers and melt-free glacier ice.

The records of black carbon and dust (Figure 5a, b) provided a preliminary age-scale for the entire core, but there is some ambiguity in certain sections of these records. For this reason, incorporating lead into the dating scheme proved valuable, as extremely low background values of lead provide an independent marker for winter snow (Figure 5c). Additionally, the dated lead time series corresponds well with known histories of lead emissions from North America, giving us confidence in the accuracy of our dating (see below). The extreme lead concentrations in the deepest 20 m of the core correspond with the 1970s, when leaded gasoline use in the United States and Canada was near its maximum.

Subsequent regulation by both countries halved the amount of lead in gasoline in 1982, and eliminated it altogether by the early 1990s (Bülhofer and Rosman, 2001). We see this decrease in lead at Combatant Col, with concentrations sharply dropping off in the early 1980s and remaining low through the 1990s.

Comparison with lead records from two other ice-cores also suggests that our dating is sound, and provides the additional information that lead aerosol deposited at Combatant Col is primarily from North American sources, in contrast to the interpretation of lead deposition in the Mt. Logan ice-core record (Osterberg and others, 2008). Figure 6 shows annual lead concentrations from four sites: Combatant Col (Figure 5a), southwest Greenland ACT2 (Figure 6a; 66.0º N, 45.2º W, 2410 m; McConnell and Edwards, 2008), Greenland Summit (Figure 6a; 72.6° N, 38.5° W, 3210 m; J. McConnell, unpublished), and Mt. Logan Prospector-Russell Col (Figure 6b; 60.6° N, 140.6° W, 5300 m; Osterberg and others, 2008). The Combatant Col lead record correlates well with both the Greenland ACT2 (period 1972-1998, $r = 0.82$, $p < 0.02$) and Greenland Summit (period 1972-2009, $r = 0.62$, $p < 0.02$) lead records. Consistent with this correlation, lead-isotope data indicate that North America is the dominant source of lead in Greenland (Rosman and others, 2000). There is no significant correlation between the Combatant Col and Mt. Logan lead records.

Water stable-isotopes, $\delta^{18}O$ and δD, were the final component included in our multi-parameter dating of the Combatant Col ice-core. For the purposes of dating, $\delta^{18}O$ and δD are nearly identical, so we report only $\delta^{18}O$ here (Figure 5d). The initial time scales, based on visual and chemical stratigraphy only, agree well with the $\delta^{18}O$ data. Data from the shallow ice-core drilled at the site in 2006 provide additional, definitive validation for our dating of the most recent five years of the 2010 ice-core (see Figure 7). In the 2006 core, the top of

which represents the snow surface during summer of that year, we see anomalously negative $\delta^{18}O$ (-29.58‰) 2.3 m below the surface, deposited during winter 2005-2006 or spring 2006. This same 2006 annual-layer from the more recent and longer Combatant Col ice-core, now buried at a depth of ~36 m, exhibits nearly identical minimum values—the most negative of the entire record. We are confident that these are the same annual-layer, and we further note that the $\delta^{18}O$ values are well-preserved at depth, showing no evidence of alteration of the original surface layers deposited in 2006 through the subsequent five years. This is significant, because alteration of water stable-isotopes, including diminished seasonality and an overall decrease in summertime values, is commonly observed even at cold glacier sites (Koerner, 1997; Moran and Marshall, 2009). In the Combatant Col core, we observe seasonal isotope variation of roughly constant amplitude throughout the record, including in the deepest ice.

Annual-layer thickness and ice-flow corrections

Annual-layer thicknesses from the Combatant Col ice-core (Figure 8) indicate extremely thick snow and ice sequences from the most recent (and least flow-altered) layers at the site, up to 12 m ice-equivalent at the thickest. These layers gradually thin with depth, due to ice-flow, to reach annual-layer thicknesses of 1-2 m ice-equivalent at depths below ~100 m. We calculate uncertainties in layer thickness by considering the standard error of the thicknesses from four sequentially developed age scales.

To obtain annual accumulation rates, we correct annual layer thicknesses for dynamic thinning using the one-dimensional ice-flow model of Dansgaard and Johnsen (1969). This model uses a simple piecewise-linear approximation of the horizontal-velocity

profile, assumed to be constant at value u_s from the surface down to some distance h above the bed, and then decreasing linearly towards a value u_b, which is the sliding velocity, at the bed. The depth-age relation for constant accumulation and steady state flow is given as follows, where H is the total ice thickness, $\dot{b}$ is the sum of the surface accumulation rate and the basal melt rate, u_s is the surface velocity, and z is the distance above the bed.

$$t(z) = \frac{H}{u_s \dot{b}} \ln \frac{h(u_b - u_s) + 2u_s z}{h(u_b - u_s) + 2u_s} \qquad z > h$$

$$t(z) = \frac{2H}{u_s \dot{b}} \ln \frac{(u_b - u_s)h + 2u_s h}{(u_b - u_s)h + 2u_s} \qquad z = h$$

$$t(z) = t(h) + \frac{H}{u_b \dot{b}} \left(\ln \frac{z}{(u_b - u_s)z - 2u_b h} - \ln \frac{h}{(u_b - u_s)h - 2u_b h} \right) \qquad z < h,\ u_b > 0$$

$$t(z) = \frac{2H}{u_s \dot{b}} \left(1 - \frac{h}{z} \right) \qquad z < h,\ u_b = 0$$

Assuming that there is no long-term trend in accumulation rate, we can estimate the parameter h and the ratio u_b/u_s by minimizing the difference between the calculated and observed age-depth relationship over a range of plausible values of surface accumulation rate $\dot{b}$ and total ice thickness, H. That is, we minimize the root mean square difference $\sqrt{\sum \left(t_m(z) - t(z) \right)^2}$ where t_m is the measured timescale and t is the calculated timescale at ice-equivalent heights z. Note that although it is virtually certain that there is melting at the bed, it is negligible in this setting even at very high geothermal heat flux, because the surface accumulation rate is so high. For example, a geothermal heat flux of 120 mW m^{-2}, about twice the regional average (e.g. Lewis et al., 1985), would result in basal melt rates of

order only 1 cm a^{-1} (e.g. Paterson, 1994); thus $\dot{b}$ is approximated simply by the surface accumulation rate.

The results show that lowest *rms* values are found with $\dot{b}$ ~ 7 m a^{-1} and H ~ 240 m (ice equivalent), both very consistent with the observations. As shown in Figure 9a, optimal values of h/H and u_b/u_s are h/H ~ 0.6-0.7, u_b/u_s < 0.1, consistent with typical values for flow near an ice divide (Waddington et al., 2001). We note that somewhat lower *rms* values can be obtained for $\dot{b}$ = 8 m a^{-1} and H = 260 m, if h/H is >0.9. However, H > 250 m is unlikely on the basis of the radar data (Figure 3a), although it cannot be ruled out. Basal sliding rates greater than u_b/u_s = 10% would also require ice thicknesses that are likely ruled out by the radar data, strongly indicating that basal sliding is a small fraction of the total sliding. In any case, corrections to the annual layer thickness using a range of plausible choices are essentially identical to those for $\dot{b}$ = 7 m a^{-1} and H = 240 m, because higher accumulation rates and/or high sliding rates require greater thinning at depth (and therefore a greater value of h/H) to be consistent with the observations. Conversely, low values of accumulation rate imply smaller values of H and h/H. However, depths <230 m are inconsistent with the observed depth-age relationship, regardless of the values of h/H and u_b/u_s used. We conclude that the observed depth-age relationship strongly constrains the layer-thinning profile with depth, allowing us to convert the measured layer thicknesses to original annual accumulation rates at the surface. For simplicity, we use $\dot{b}$ = 7 m a^{-1}, h/H = *0.65,* H = 240 m, and u_b/u_s = 0. Figure 9b compares the calculated timescale for these parameters, compared with the observations. Note that the implied age at depth is well in excess of 200 years; we discuss the implications of this for future work later in this paper.

The time series of ice flow-corrected net annual accumulation from Combatant Col is shown in Figure 10. Maximum annual accumulation rates of 10-11 m a^{-1} ice-equivalent are observed, with minima no lower than ~4 m a^{-1}. Annual accumulation rates of this magnitude, averaging 6.8 m a^{-1} over this 38-year record, place Combatant Col among the wettest places on Earth (see National Climatic Data Center, 2008). Accumulation at the site shows a standard deviation of 1.64 m, which eclipses entire annual average precipitation rates at nearby coastal weather stations. For instance, lee-side stations on Vancouver Island average annual precipitation of 1.0-1.5 m a^{-1} from 1971-2000 (Environment Canada, 2011). We estimate uncertainty in the accumulation data by taking into account estimated uncertainty in the timescale, based on the sequence of four depth-age relationships developed iteratively as individual stratigraphic time series (i.e. records of melt layers, geochemistry, isotopes) were incorporated into our multiparameter dating (described in "Dating" section above). This translates to an average uncertainty of ~12% in accumulation for each year, or, equivalently, an age uncertainty of ~1 year.

Relationship between accumulation rate at Combatant Col and regional precipitation

Time series of annual snow accumulation developed from alpine ice-core records have been used previously as indicators of past climate variability. A central challenge to using ice-core records in this way, however, is that the accumulation rate at a specific high-altitude site may reflect only very regional climate, or even microclimatic conditions. Nevertheless, previous studies have had some success: the Mt. Logan accumulation time series has been used to examine variability in the strength of the Aleutian Low (e.g. Moore and others, 2003), although Rupper and others (2004) argued that the Mt. Logan record

could be meaningfully related to the large-scale precipitation variability only for the largest winter storms. A longer record from Combatant Col could potentially be used to extend observations of such variability well beyond the length of the instrumental climate record. While it is beyond the scope of this paper to examine the controls on regional precipitation region in detail, it is nevertheless of interest to examine the extent to which the Combatant Col record may similarly reflect regional or large-scale climate variability.

Comparison with both local precipitation records (sites shown in Figure 1) and large-scale climate reanalysis suggests that the Combatant Col record does meaningfully reflect regional-scale precipitation. We calculated the correlation between the annually-averaged accumulation from Combatant Col and the annual mean precipitation rates from British Columbia weather stations (Environment Canada, 2011), using seasonal (3-month) averages for all seasons, starting in July (the nominal beginning of each accumulation year in the core), for lags of up to one year (Figure 11). We find that correlations are maximized with a lag of one year, and are statistically highly significant at that lag ($p < 0.05$ to $p < 0.01$, accounting for autocorrelation in the data following Bretherton and others, 1999). Although a lag of one year is obviously not physically meaningful, this lies within the expected dating uncertainty for the core. Furthermore, if this is correct, it provides confirmation that the dating of this core is incorrect by only one year. Although we cannot fully rule out chance correlations, several lines of evidence argue that this reflects a real, physically meaningful relationship between Combatant Col accumulation and regional precipitation. First, the maximum correlation occurs when the station averages are centered on the winter accumulation season, November though January. Second, significant correlations are found only with the weather station records to the west of the Coast Mountains—at Port Hardy,

Tofino, and Campbell River on Vancouver Island, plus Powell River on the mainland (Figure 11c)—and not with stations further to the east, north or south (e.g. Tatlayoko, Prince Rupert, Lillooet; see Figure 11c). This pattern of correlation is to be expected, because Mt. Waddington clearly receives precipitation almost exclusively due to orographic effects as westerly storms encounter the Coast Mountains, rather than from easterly flow originating in the dry British Columbia interior. Finally, we find that if we shorten the total length of the record by one year, by combining the annual accumulation total of two randomly-chosen adjacent years (e.g. the 5.9 m in 2004 and 7.4 m in 2005 becomes 13.3 m in 2005)—a reasonable possibility as annual stratigraphy in some years is not entirely unambiguous—significant correlations remain, but with zero lag.

Further evidence that the Combatant Col time series meaningfully reflects large-scale precipitation variability is found in the relationship with regional precipitation and geopotential heights as determined from the ERA40/ERA-Interim climate reanalysis data (Upalla and others, 2005; Dee and others, 2011). We find that for one-year averages of Combatant Col accumulation, the correlations for both precipitation and 500 hPa geopotential heights are not significant ($p > 0.1$). However, if 3-year averages are used (to account for possible dating uncertainty) significance levels are moderately high ($p<0.1$) where expected: over Mt. Waddington itself, and over Vancouver Island to the immediate west (see Figure 12). Furthermore, the correlation pattern with both precipitation and 500 hPa geopotential heights is consistent with previous understanding of large-scale controls on precipitation variability in this region (Overland and Hiester, 1980). In particular, positive correlations with precipitation extend westward along the climatological trajectory of westerly wind, while there is a negative correlation with precipitation in coastal Alaska,

similar to the characteristic South-North dipole pattern associated with the Pacific/North American pattern (Wallace and Gutzler, 1981). The correlation with 500 hPa geopotential height is characterized by negative correlation (associated with low geopotential heights) over the Gulf of Alaska, and positive correlations (associated with higher than average geopotential heights) over the Aleutians (moderately significant at $p < 0.1$). This is the configuration of geopotential height associated with greater than average storminess and precipitation along the west coast of British Columbia (Rodionov and others, 2007).

These correlations are based on a relatively short record, only 38 years, while the ultimate goal of this ice-core project is to gain insight into regional conditions extending beyond the instrumental period. This should be achievable at Combatant Col, because, as suggested above, ice ages in excess of 200 years near the bed are very likely based on our current knowledge of depth-age relationships at the ice-core site. Additionally, a longer record should allow for more precise dating, because the age of deeper ice would likely be constrained by deposits from the Katmai, Alaska (1912), and Tambora, Indonesia (1815) eruptions, which are seen in the Eclipse Icefield and other ice-cores (Yalcin and Wake, 2001).

Conclusions

Retrieving ice-core paleoclimate records from temperate glaciers has been attempted only rarely, because it has often been observed, and consequently often assumed, that annual stratigraphy—critical to dating the records—will not be preserved. Our results from the Combatant Col ice-core demonstrate that annual-layers can be preserved in temperate ice, provided that annual snow accumulation rates exceed the depth penetrated by summer surface meltwater. In addition to allowing for accurate dating, preserved chemical

stratigraphy provides valuable information about the deposition of natural and anthropogenic aerosols at remote sites (e.g. McConnell and others, 2007). Furthermore, the accumulation time series from the Combatant Col ice-core appears to meaningfully reflect regional-scale climate variability. These results suggest that there is more potential than previously thought in exploring additional ice-core sites at mid-latitudes where cold glaciers are relatively rare. Although the high-accumulation criterion limits the age of ice preserved at depth in relatively shallow alpine glaciers, ice with an age of several hundreds of years is likely preserved at Combatant Col. A deeper ice-core from this site would complement other existing ice-core records in the North Pacific, and would add much-needed spatial detail to the study of regional climate variability on decadal to centennial scales.

Acknowledgements

We thank Beth Bergeron and Ice Drilling Design and Operations for expert drilling leadership, the King family and employees at White Saddle Air, Bluff Lake, British Columbia, and TC Trans trucking for an emergency ice-core freezer replacement. Field assistants were M. Bisiaux, N. Bowermann, K. Sterle, J. Theis, S. Schoenemann, A. McKee, M. Park, T. Hutchison, J. Brann and K. McConnell. H. Roop assisted in planning field logistics, and helped process the core along with A. Gusmeroli. T.J. Fudge assisted in dating of the core. We also thank the National Ice Core Laboratory for sampling support, and technicians and students at the Desert Research Institute Ultra-Trace Chemistry Laboratory and University of Washington Stable-isotope Laboratory (Δ*IsoLab) for their analytical expertise. E.D. Waddington and G. Roe provided helpful comments on the manuscript. This project was

supported by grants from the U.S. National Science Foundation Paleoclimate Program, award numbers 0902240, 0902392, 0902734, and 0903124.

REFERENCES

Bey I and 3 others (2001) Asian chemical outflow to the Pacific in spring: Origins, pathways, and budgets. *J. Geophys. Res.*, **106**, D000806. (0148-0227/01/2001JD000806.)

Bretherton CS and 4 others (1999) The effective number of spatial degrees of freedom of a time-varying field. *J. Clim.*, **12**(7), 1990-2009.

Bulhöfer A and Rosman KJR (2001) Isotopic source signatures for atmospheric lead: The Northern Hemisphere. *Geochim. Cosmochim. Acta*, **65**(11), 1727-1740.

Dansgaard W and Johnsen SJ (1969) A flow model and a time scale for the ice core from Camp Century, Greenland. *J. Glaciol.*, **8**(53), 215–223.

Dee DP and 35 others (2011) The ERA-Interim reanalysis: configuration and performance of the data assimilation system. *Q. J. R. Meteorol. Soc.*, **137**, 553-597. DOI:10.1002/qj.828

Environment Canada (2011) Canadian climate normals 1971-2000. *National Climate Data and Information Archive*. www.climate.weatheroffice.gc.ca.

EPICA community members (2004) Eight glacial cycles from an Antarctic ice core. *Nature*, **429**, 623-628.

Fisher DA and 12 others (1998) Penny Ice Cap cores, Baffin Island, Canada, and the Wisconsinan Foxe Dome connection: two states of Hudson Bay ice cover. *Science*, **279** (5351), 692-695.

Fisher DA and 16 others (2008) The Mt Logan Holocene-late Wisconsinan isotope record: tropical Pacific-Yukon connections. *The Holocene*, **18**(5), 667-677.

Ice Drilling Design and Operations (2011) *Long Range Drilling and Technology Plan*. University of Wisconsin, Madison. Ice Drilling Program Office. http://icedrill.org/documents/view.shtml?id=272.

Jaffe D and 3 others (2003) Six 'new' episodes of trans-Pacific transport of air pollutants. *Atmos. Envir.,* **37**(3), 391-404.

Koerner RM (1997) Some comments on climatic reconstructions from ice cores drilled in areas of high melt. *J. Glaciol.*, **43**(143), 90-97.

Lewis TJ, Jessop AM and Judge AS (1985) Heat flux measurements in southwestern British Columbia: the thermal consequences of plate tectonics. *Canadian Journ. of Earth Sci.*, **22**(9), 1262-1273.

Lliboutry L (1971) Permeability, brine content and temperature of temperate ice. *J. Glaciol.*, **10**(58), 15-29.

McConnell JR and 3 others (2002) Continuous ice-core chemical analyses using inductively coupled plasma mass spectrometry. *Envir. Sci. Technol.*, **36**(1), 7-11.

McConnell JR and 9 others (2007) 20th-century industrial black carbon emissions altered Arctic climate forcing. *Science*, **317**, 1381-1384.

McConnell JR and Edwards R (2008) Coal burning leaves toxic heavy metal legacy in the Arctic. *Proceedings of the National Academy of Sciences*, doi:10.1073/pnas.0803564105

McGwire KC and 6 others (2008) An integrated system for optical imaging of ice cores. *Cold Reg. Sci. Technol.*, **53**(2), 216-228.

Merrill JT, Uematsu M and Bleck R (1989) Meterological analysis of long range transport of mineral aerosols over the North Pacific. *J. Geophys. Res.*, **94**, D00089. (0148-0227/89/89JD00089.)

Moran T and Marshall S (2009) The effects of meltwater percolation on the seasonal isotopic signals in an Arctic snowpack. *J. Glaciol.*, **55**(194), 1012-1024.

Naftz DL and 7 others (1996) Little Ice Age evidence from a south-central North American ice core, U.S.A. *Arc. and Alp. Res.*, **28**(1), 35-41.

National Climatic Data Center (2008) Global measured extremes of temperature and precipitation. *U.S. Dept. of Commerce*. http://www.ncdc.noaa.gov/oa/climate/globalextremes.html#sites. Accessed March 1, 2012.

Osterberg E and 10 others (2008) Ice core record of rising lead pollution in the North Pacific atmosphere. *Geophys. Res. Lett.*, **35**, L05810. (10.1029/2007GL032680.)

Overland JE and Hiester TR (1980) Development of a synoptic climatology for the Northeast Gulf of Alaska. *J. Appl. Met.*, **19**(1), 1-14.

Paterson WSB (1994) *The Physics of Glaciers*, 3rd ed., 481pp., Elsevier, Amsterdam.

Preunkert S and 3 others (2000) Col du Dôme (Mont Blanc Massif, French Alps) suitability for ice-core studies in relation with past atmospheric chemistry over Europe. *Tellus*, **52B**, 993-1012.

Rodionov SN, Bond NA and Overland JE (2007) The Aleutian Low, storm tracks, and winter climate variability in the Bering Sea. *Deep Sea Res. II*, **54**, 2560-2577.

Rosman KJR and 4 others (1994) Isotopic evidence to account for changes in the concentration of lead in Greenland snow between 1960 and 1988. *Geochim. Cosmochim. Acta*, **58**(15), 3265-3269.

Rupper S, Steig EJ and Roe G (2004) The relationship between snow accumulation at Mt. Logan, Yukon, Canada, and climate variability in the North Pacific. *J. Climate*, **17**(24), 4724-4739.

Schotterer U and 3 others (1997) Isotope records from Mongolian and Alpine ice cores as climate indicators. *Climatic Change*, **36**, 519-530.

Schotterer U, Stichler W and Ginot P (2004) The influence of postdepositional effects on ice core studies: examples from the Alps, Andes, and Altai. *In* Cecil, L.D., J.R. Green and L.G. Thompson, *eds. Earth paleoenvironments: records preserved in mid- and low-latitude glaciers*. Dordrecht, etc., Kluwer Academic, 39-60.

Schwikowski M and 3 others (1999) A high-resolution air chemistry record from an Alpine ice core: Fiescherhorn glacier, Swiss Alps. *J. Geophys. Res.*, **104**, D100112. (0148-0227/99/1998JD100112).

Shiraiwa T and 7 others (2003) Ice core drilling at King Col, Mount Logan 2002. *Bull. Glaciol. Res.*, **20**, 57-63.

Taylor KC and 12 others (1997) The Holocene-Younger Dryas transition recorded at Summit, Greenland. *Science*, **278**, 825-827.

Thevenon F and 3 others (2009) Mineral dust and elemental black carbon records from and Alpine ice core (Colle Gnifetti glacier) over the last millennium. *J. Geophys. Res.*, **114**, D17102. (10.1029/2008JD011490).

Thompson LG (2004) High-altitude, mid and low-latitude ice core records: implications for our future. *In* Cecil, L.D., J.R. Green and L.G. Thompson, *eds. Earth paleoenvironments: records preserved in mid- and low-latitude glaciers*. Dordrecht, etc., Kluwer Academic, 3-15.

Uppala SM and 45 others (2005) The ERA-40 re-analysis. *Q. J. R. Meteorol. Soc.*, **131**, 2961-3012. DOI: 10.1256/qj.04.176

Urmann D (2009) Decadal scale climate variability during the last millennium as recorded by the Bona Churchill and Quelccaya ice cores. PhD thesis, Ohio State University, Columbus.

Vincent C and 4 others (1997) Snow accumulation and ice flow at Dôme du Goûter (4300m), Mont Blanc, French Alps. *J. Glaciol.*, **43**(145), 513-521

Waddington ED, Bolzan JF and Alley RB (2001) Potential for stratigraphic folding near ice-sheet centers. *J. Glaciol.,* **47**(159), 639-648.

Wallace JM and Gutzler DS (1981) Teleconnections in the geopotential height field during the Northern Hemisphere Winter. *Mon. Wea. Rev.*, **109**, 784-812.

Yalcin K and Wake CP (2001) Anthropogenic signals recorded in an ice core from Eclipse Icefield, Yukon Territory, Canada. *Geophys. Res. Lett.,* **28**(23), 4487-4490.

Yasunari TJ and 7 others (2007) Intra-annual variations in atmospheric dust and tritium in the North Pacific region detected from an ice core from Mount Wrangell, Alaska. *J. Geophys. Res.*, **112**, D10208. (10.1029/2006JD008121.)

FIGURES

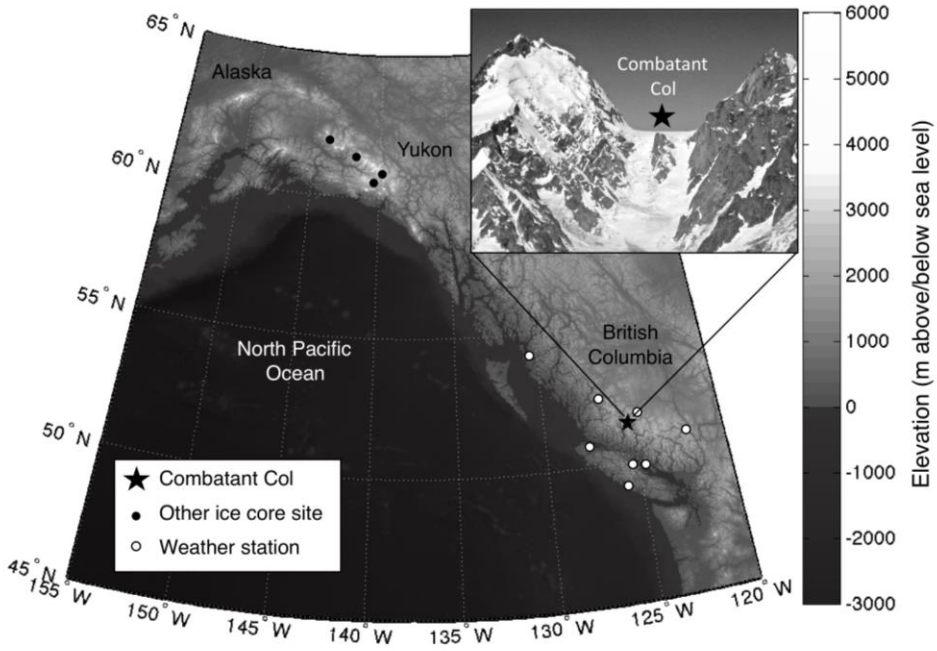

Figure 1. Map location of Combatant Col drill site (starred), with inset picture showing local setting (E. Steig photo). Other ice cores and weather stations mentioned in the text are marked by black and white circles, respectively.

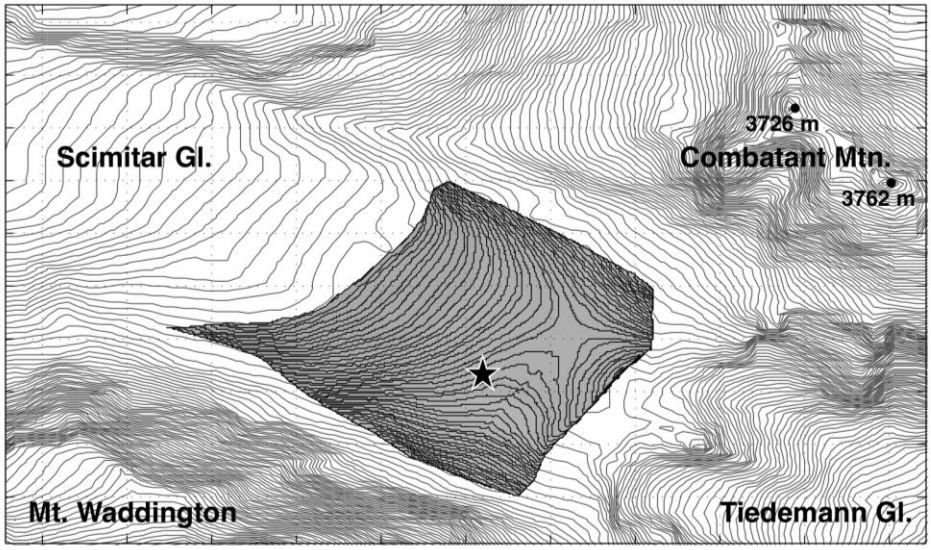

Figure 2. Detail of drill site (starred) and ice-surface topography. Gray lines show 20 m digital-elevation map (DEM) data. Black contours in the shaded area are derived from GPS surveys conducted during field campaigns and are plotted with a 2 m contour interval. These new surface-elevation data correct 20-40 m errors in the original 20m DEM at Combatant Col.

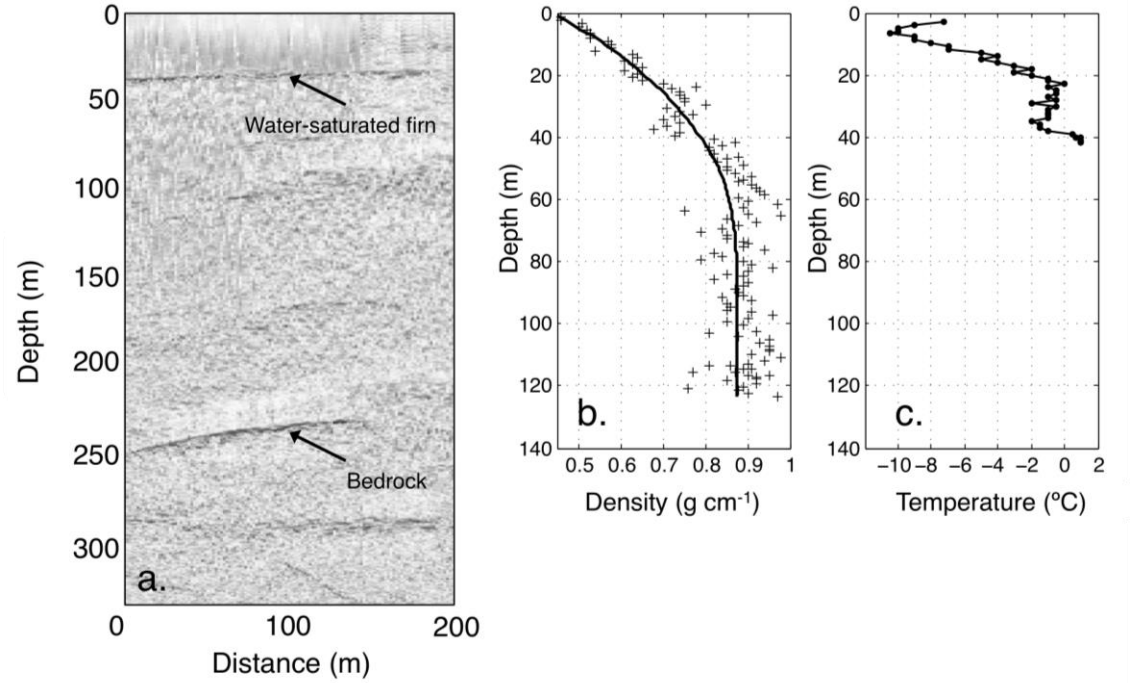

Figure 3. a) Radar data (80 MHz center frequency) from a transect across the center of Combatant Col, perpendicular to ice flow. Arrows indicate the location of water-saturated firn, near 40m depth, and a bedrock reflector at ~250m. b) Ice-core density measurements, made in the laboratory, fit with a 3rd-order polynomial used to calculate ice-equivalent

depths. The firn-ice transition at 830 g cm^{-3} occurs at a depth of ~45 m. c) Ice-core temperature, measured in the field, shows ice reaching ~0ºC at a depth of 40 m.

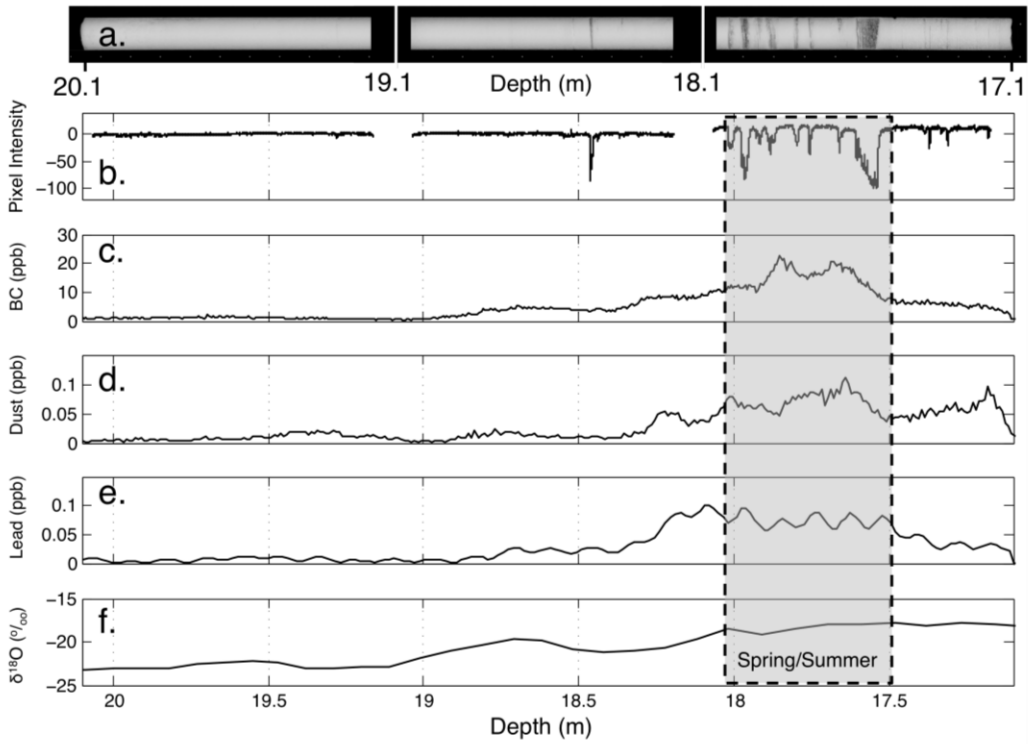

Figure 4. Example section from 17 to 20 m depth in the combatant Col ice core, depicting seasonality in records of a) visual appearance, b) pixel intensity (melt layers, c) black carbon (BC), d) dust, e) lead, and f) $\delta^{18}O$. All data show lower concentrations/values during winter, gradually increasing to a spring/summer maximum, highlighted by grey box.

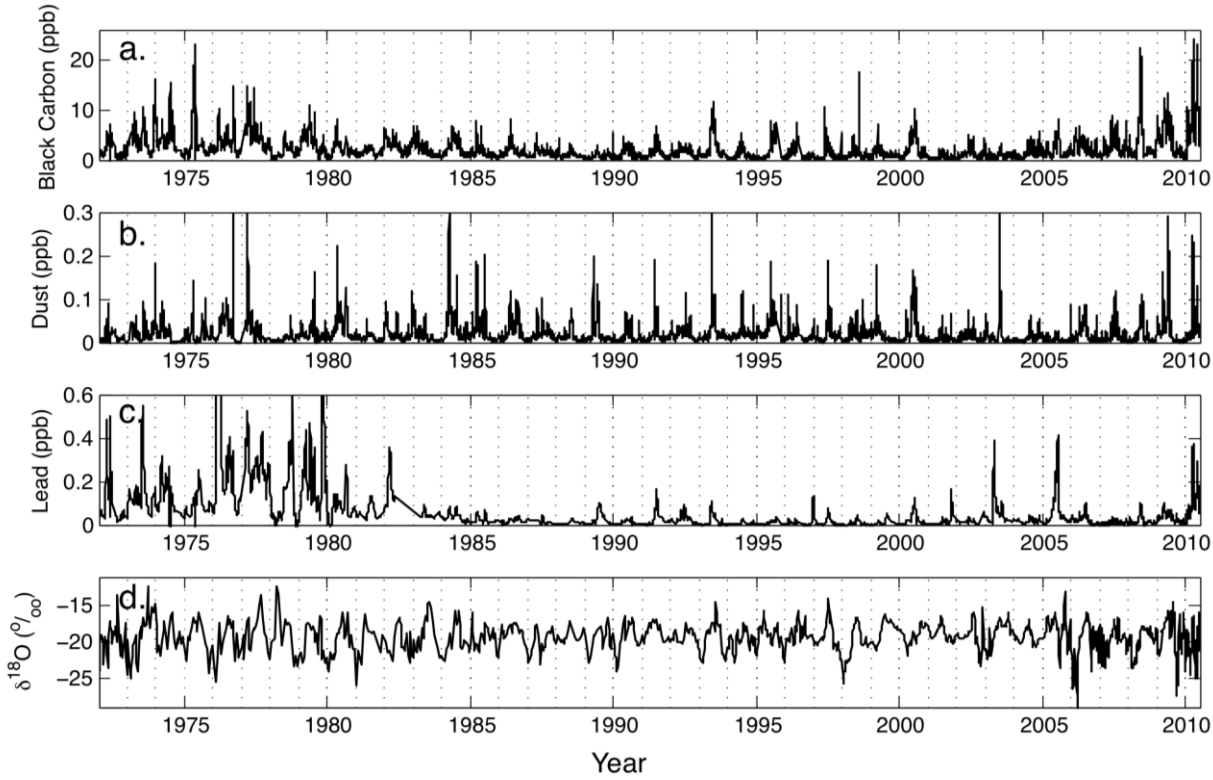

Figure 5. Concentrations of a) black carbon, b) dust, c) lead and d) $\delta^{18}O$ in the Combatant Col ice core, plotted vs. age.

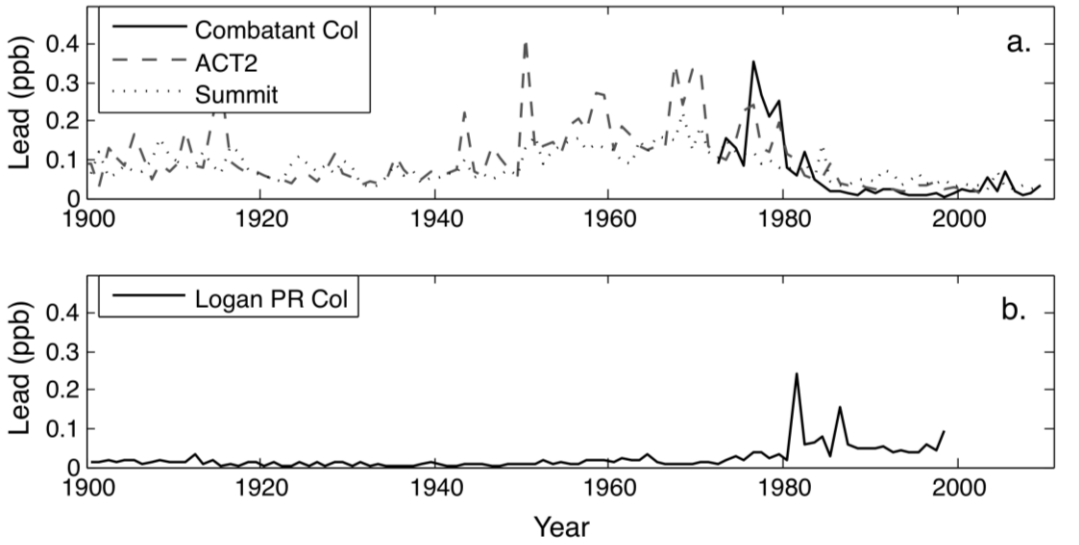

Figure 6. Comparison between Combatant Col annual lead concentrations (a, black line) and ice-core lead records from the Greenland Ice Sheet (a, dotted and dashed lines) and Mt. Logan PR Col (b). Both the Combatant Col and Greenland ACT2 (dashed line) and Summit (dotted line) records show high lead concentrations in the 1970s, followed by sharp decreases in concentration in the early 1980s. In contrast, lead concentrations at Mt. Logan show a steady rise from the 1970s to the most recent years of the record.

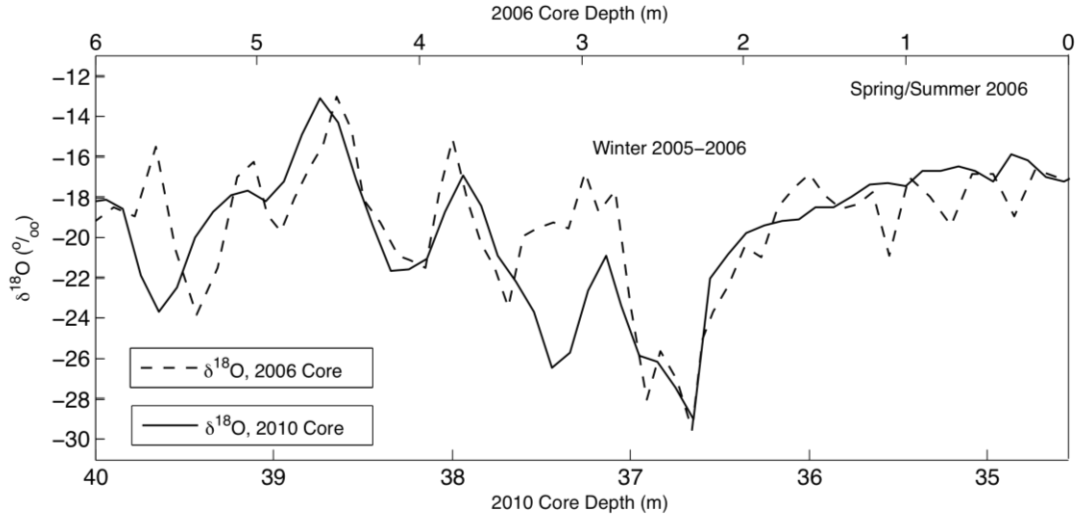

Figure 7. Comparison of $\delta^{18}O$ in the 2006 and 2010 cores. The nearly identical extreme minimum in $\delta^{18}O$, dating to winter 2005-2006, demonstrates the preservation of seasonality through firn and into ice.

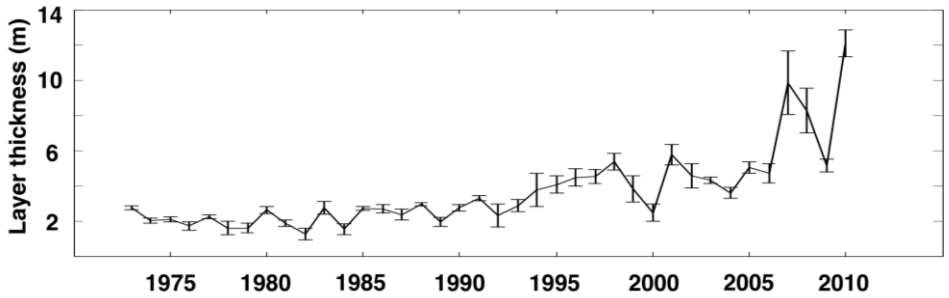

Figure 8. Annual layer thickness from the Combatant Col ice core record. Error bars indicate ± one standard error calculated from four agescales (see text for details).

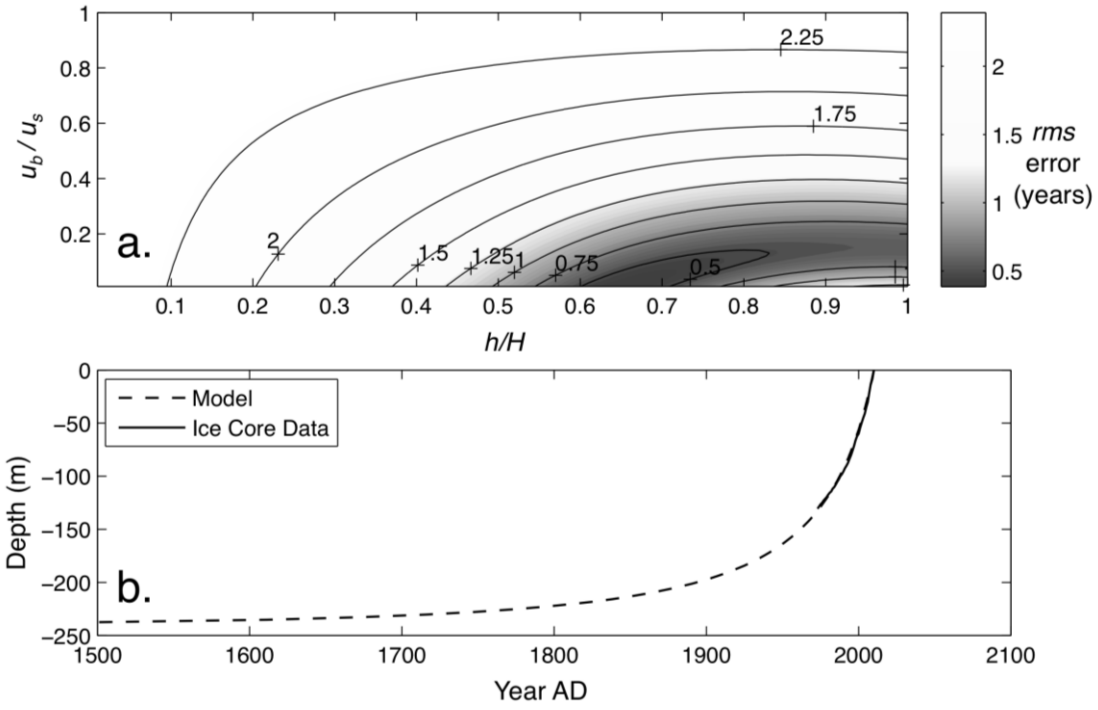

Figure 9. a) Root mean square difference between measured depth-age relationship for the Combatant Col core and that calculated with a Dansgaard-Johnsen flow model for all possible values of h/H and of u_b/u_s. b) Measured and modeled depth-age relationships, using $u_b/u_s = 0$, $h/H = 0.65$, $\dot{b} = 7$ m a^{-1} and $H = 240$ m.

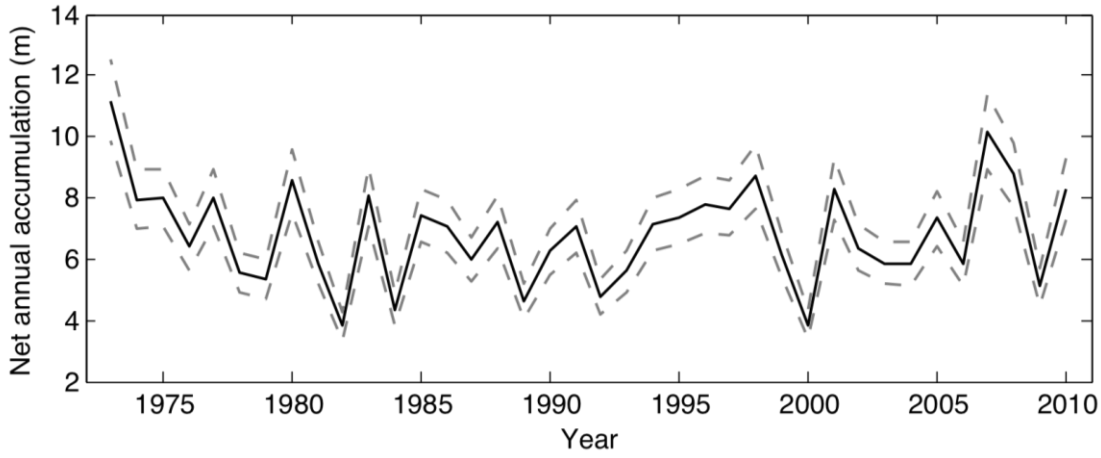

Figure 10. Ice-flow-corrected annual accumulation, with a ± 12% uncertainty threshold marked by the gray dashed lines.

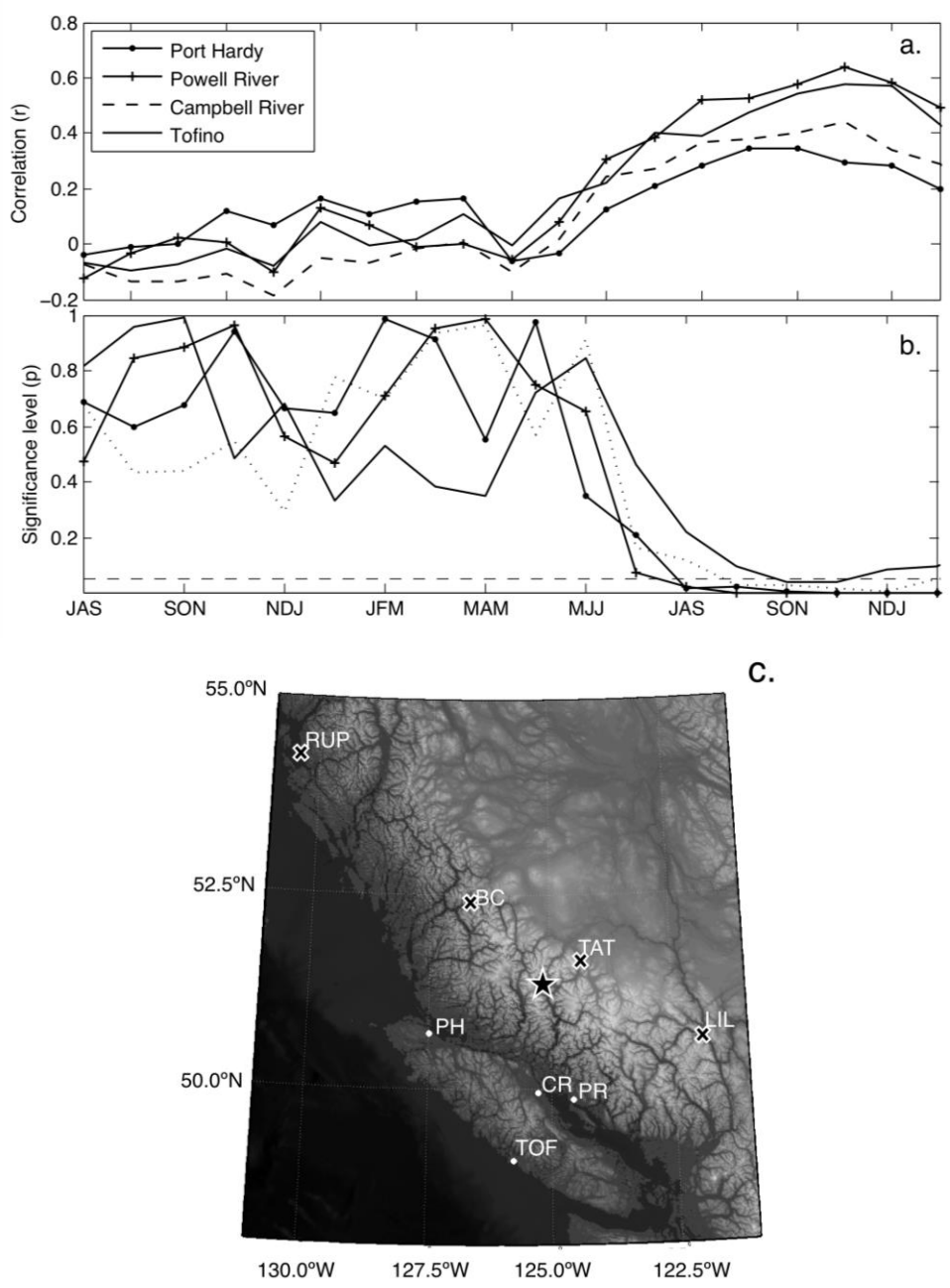

Figure 11. Correlation between Combatant Col accumulation timeseries and precipitation data from nearby weather station precipitation data (a). Significance levels are plotted in (b), indicating that with ~1 year offset correlations become statistically significant between Combatant Col accumulation and weather-station precipitation data. Map (c) shows weather stations used for precipitation data: Port Hardy (PH), Campbell River (CR), Tofino (TOF), Powell River (PR), Prince Rupert (RUP), Bella Coola (BC), Tatlayoko Lake (TAT), and Lillooet (LIL). Weather stations that correlate with Combatant Col accumulation data are marked with white circles; those that show no correlation are marked with a black 'x'. Combatant Col is starred.

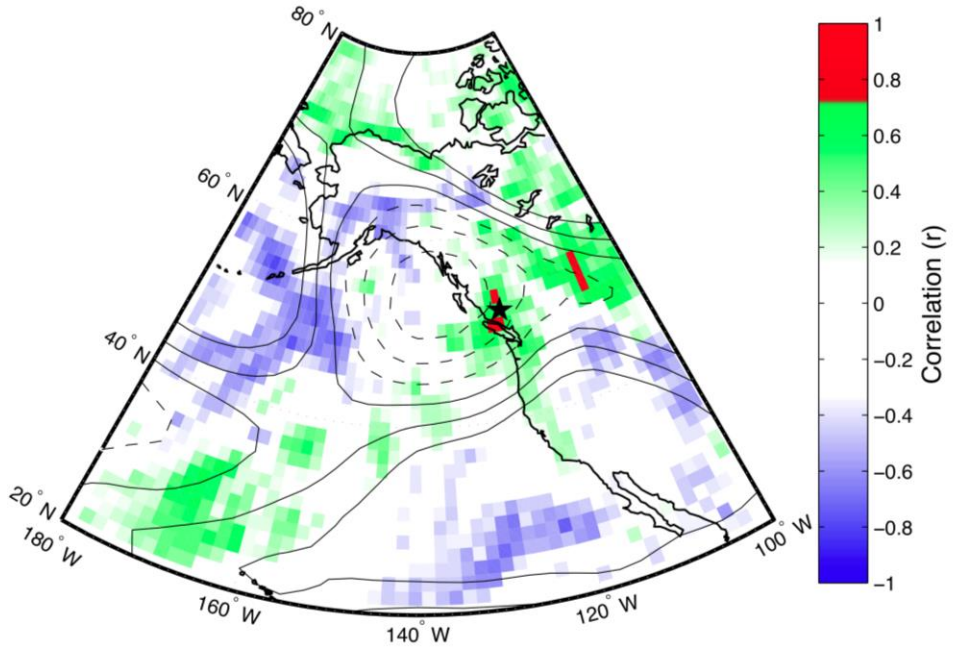

Figure 12. Correlation between Combatant Col accumulation and ERA-40/ERA-Interim precipitation and 500hPa geopotential heights. Colors indicate correlation (r) with precipitation. Contours indicate correlation with 500 hPa geopotential height (contour interval is 0.1, with zero and negative values dashed). Combatant Col location is starred.